Breeze analysis by mast and sodar measurements (*)(**)

G. LEUZZI and P. MONTI
Facoltà di Ingegneria, Università degli Studi "La Sapienza"
Via Eudossiana 18, 00184 Roma, Italy

(ricevuto il 10 Gennaio 1996; revisionato il 10 Luglio 1996; approvato il 15 Luglio 1996)

Summary. — During the year 1993, field measurements were carried out in a meteorological station located in the neighbourhood of Rome, 10 km from the coast (Tyrrhenian Sea). The monitoring station is composed of a 30 m mast and a three-axial Doppler sodar. A statistical analysis of data has been made in order to obtain the main parameters utilised by the dispersion model. Hourly, seasonal and conditional averages showed the strong influence of sea and land breeze circulation on the local characteristics of the atmospheric boundary layer. Such an aspect has to be considered in the numerical predictions of pollutant dispersion.

PACS 92.60.Fm – Boundary layer structure and processes.
PACS 01.30.Cc – Conference proceedings.

1. – Introduction

Several studies on breeze regimes have been recently carried out, either for observation of the breeze front or statistical analysis of the breeze circulation. An understanding of the sea and land breeze is useful for the evaluation of the pollutant dispersion. In papers [1, 2] the characteristics of the sea breeze front have been studied by means of turbulence probes and acoustic sounding systems. Mastrantonio *et al.* [3] investigated the inland propagation of the sea breeze through a network of Doppler sodars. A statistical description of the basic characteristics of the sea breeze has been determined in paper [4]. More recently Kaga *et al.* [5] reproduced a typical land and sea breeze field in a water tank model. This paper describes the main characteristics of breeze on a typical summer day. Furthermore, in order to provide a data base for dispersion models, a statistical analysis of the breeze regime has been carried out.

(*) Paper presented at EUROMECH Colloquium 338 "Atmospheric Turbulence and Dispersion in Complex Terrain" and ERCOFTAC Workshop "Data on Turbulence and Dispersion in Complex Atmospheric Flows", Bologna, 4-7 September 1995.
(**) The authors of this paper have agreed to not receive the proofs for correction.

2. – Site and instrumentation

The observation site is located at Ponte Malnome (41° N, 12° E), about 10 km north-east of the Tyrrhenian Sea (see fig. 1) at an altitude of 65 m a.s.l. and very close to the urban area of Rome, in a zone where some industrial plants are located. The micrometeorological station is studied for the dangerous waste incinerator of AMA (Azienda Municipalizzata Ambiente) which has been designed for the treatment of hospital waste.

The station is composed of a mast with sensors placed close to the ground level (rain, solar radiation, humidity, pressure) and at three different levels, 10, 20 and 30 m (temperature and wind velocity in all the three directions). Wind velocity is measured by Gill u, v and w propeller anemometers, temperature by thermistor probes, rain by tipping bucket raingauge, solar radiation by dome solarimeter, humidity by thin film sensor and pressure by piezoelectric cell. Signals from the sensors are converted and recorded in the memory of a data-logger every 10′, and later transferred to a PC memory.

Moreover, a three-axial Doppler sodar (APM-400 by Multimicro), which allows the measurements of velocity and turbulent characteristics of the atmospheric boundary layer (ABL), in the height range 44-889 m with a vertical resolution of about 27 m, was installed. The sodar system gives a burst with a different frequency for each antenna (1750, 2000 and 2250 Hz). The burst repetition frequency is 0.166 Hz, *i.e.* a burst every 6″ is emitted. In the configuration used the system provides the profiles of mean and variance of the wind velocities every 10′.

Data collection began on June 8, 1992, and is still in progress, but in this analysis only the year 1993 has been considered. Some information about geostrophic winds has been taken from the Pratica di Mare radiosonde station (ITAV, Meteorological Service), located near the shoreline, 24 km south of the centre of Rome.

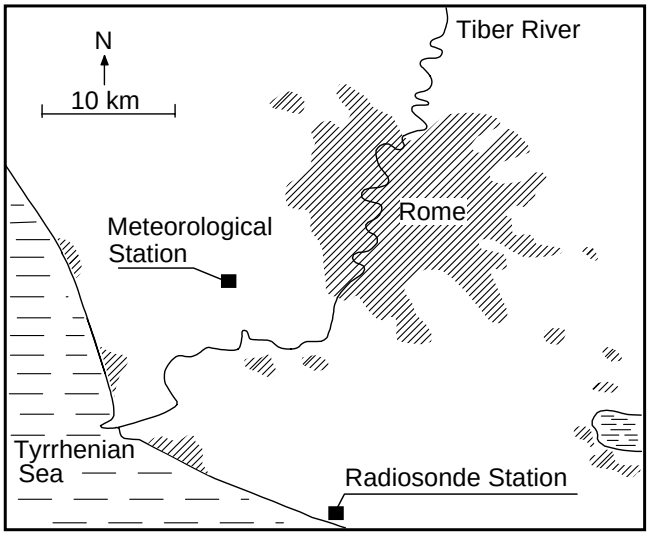

Fig. 1 – Observations site.

3. – Analysis of the sea breeze event of 3 August, 1993

In the observational site the meteorological conditions are strongly affected by sea breeze events. Such an aspect is particularly frequent during the summer. A typical diurnal cycle of the main meteorological characteristics took place on August 3. During this day high-pressure conditions are present (about 1013 mb).

In fig. 2 some of the observed variables are depicted. The data represent averaged values for a 1 hour period and are drawn at the end of every hour. The sun rises at 0508

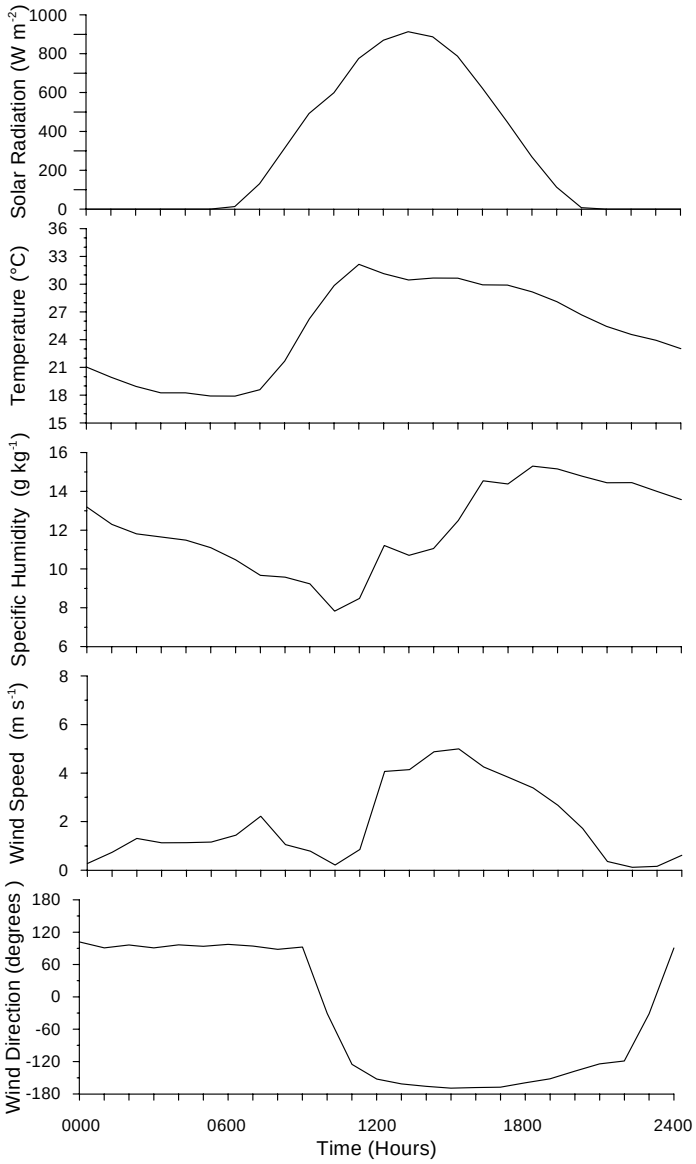

Fig. 2 – Time series of solar radiation, temperature, specific humidity, wind speed and wind direction on 3 August, 1993.

and goes down at 1951. The solar radiation reaches a maximum value of 918 W m^{-2} at 1220. In the morning the temperature increases until 1100 then, because of the sea breeze, decreases. When the sea breeze arrives the specific humidity arises and goes on to increase for the whole duration of the phenomenon. An important element in recognising the establishment of the breeze is wind speed. Its magnitude strongly increases as well as specific humidity and reaches a maximum two hours later than the solar radiation one. In the evening at 2100 the wind drops. Complementary behaviour can be observed for wind direction, which turns from 90° to −120°, perpendicular to the shore line, with a successive rotation towards south. At night-time a land breeze appears. Such a phenomenon is characterised by a wind direction of 90° and an increase in intensity, which reaches its maximum 1 hour after the sun rises. The land breeze is a dry wind, as shown by the reduction in specific humidity.

4. – Statistical analysis of the year 1993

In order to provide a data base for dispersion models, a statistical analysis of the wind characteristics and of the main parameters involved in pollutant diffusion has been carried out. Significant statistics would require an observation period of several years, nevertheless the period analysed is sufficient to describe some features of the ABL. A realistic description of pollutant dispersion requires knowledge of the whole velocity field. Diagnostic and prognostic models make it possible to evaluate the flow field if suitable boundary conditions are available. Vertical profiles of mean velocity and turbulent characteristics of the ABL are necessary for this end. Detailed information on the lowest part of the atmosphere has been obtained by mast sensors, while the above layer has been analysed by sodar.

4˙1. *Mast measurements.* – A global evaluation, including all wind velocity data, for 1993 has been carried out. Collecting all samples of the 20 m anemometers in 16 conventional sectors, the histogram on fig. 3 has been obtained. Statistics were carried out taking into consideration all the average hourly velocities and discarding those

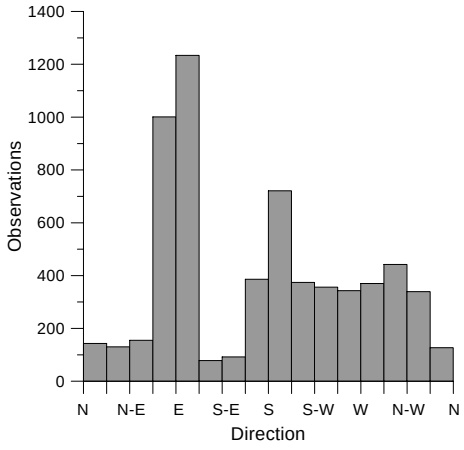

Fig. 3 – Frequencies of the wind direction.

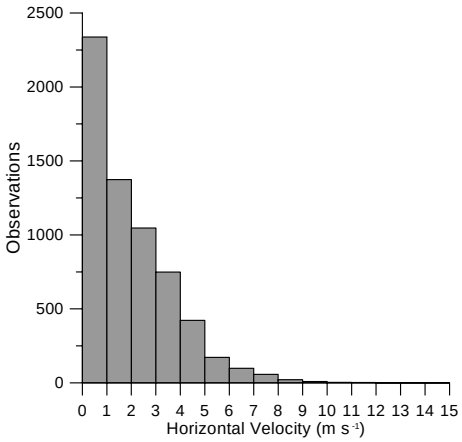

Fig. 4 – Frequencies of the horizontal velocity.

below 1 m/s, considered calm with variable directions. East winds (sector 4 and 5) are the most frequent, followed by those of the south and west sectors which, with the exclusion of the sector 9 peak, are almost equally probable. Frequency of the wind intensity is indicated in fig. 4. In most cases these winds are of weak intensity.

A more detailed analysis of wind directions has been made considering the hour and month and calculating the frequency with which the winds blow from each of the 8 sectors (with amplitude of 45°) being considered. As an example, the results of two sectors are drawn in fig. 5. Looking at the east sector (fig. 5a)), a significant number of winds in the early hours of the morning may be observed. The maxima occur before sunrise in correspondence to the land breeze events. During the winter months frequency spreads in the warmer hours. Complementary behaviour appears in the

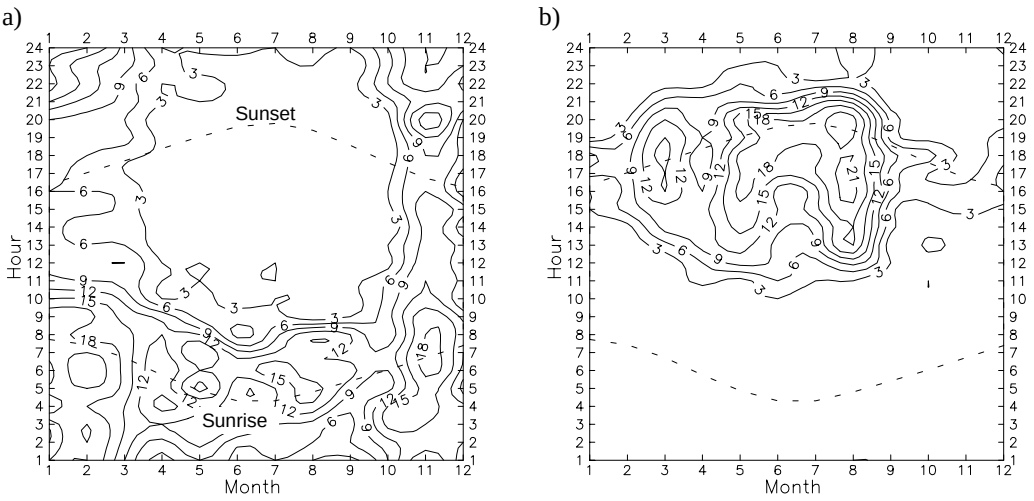

Fig. 5 – Frequency contours of the horizontal velocity; a) east wind and b) south wind.

south sector (fig. 5b)) when winds arise almost exclusively in the hottest hours of the day.

Using the information from the mast, an initial estimate has been made of the atmospheric turbulent parameters. The analysis was carried out with data available in the four quarterly periods of 1993. In these periods daily cycles of temperature, potential temperature gradient, specific humidity and velocity have been considered. Figures 6 and 7 show the summer and winter results, respectively. The temperature and humidity in fig. 6 follow the patterns observed on 3 August. On the contrary, in winter time, because of the lower influence of the sea breeze, the temperature does not register the leveling of the high values. Potential temperature gradient permits an estimate of atmospheric static stability in the layer being examined. In the case in question information is obtained on local stability near to the ground. In the winter months a local unstable condition takes place only in the interval between 1000 and 1800. This same condition occurs between 0900 and 2000 during the summer. The seasonal average of the horizontal velocity confirms once again the strong sea breeze influence but gives rise to a velocity flattening of the land breeze. Because of nocturnal

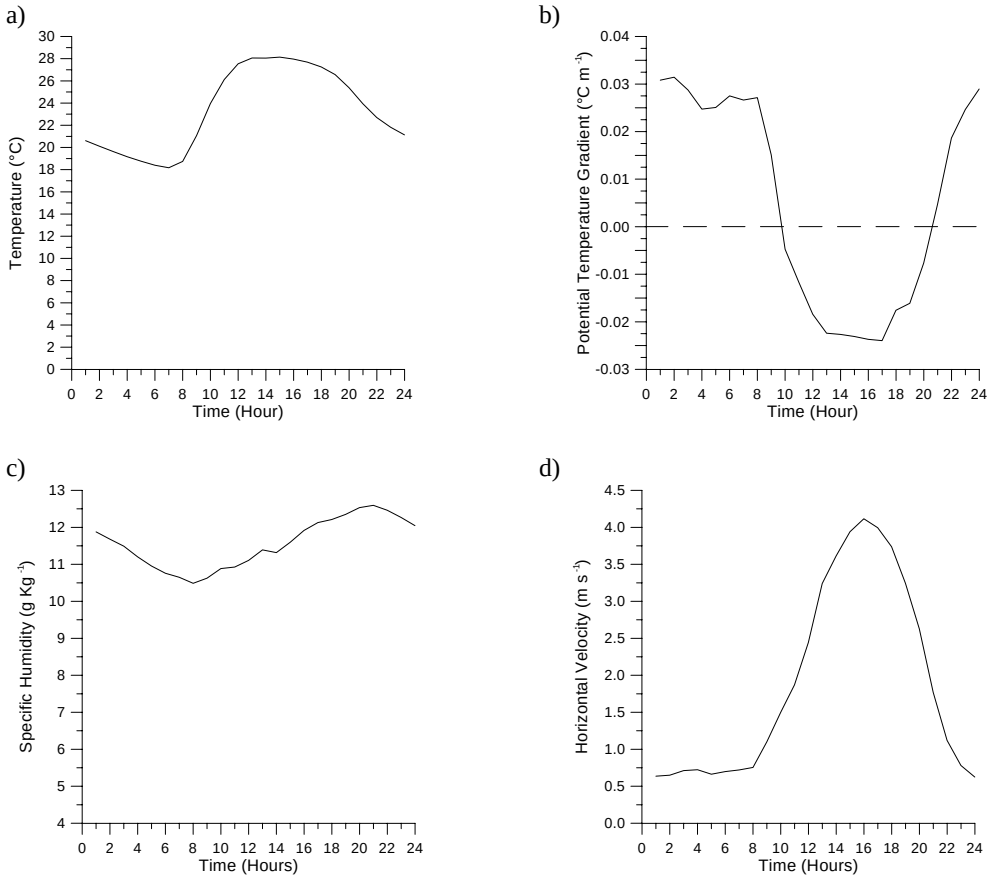

Fig. 6 – Daily cycles in the period July-September 1993; a) temperature, b) potential temperature gradient, c) specific humidity and d) horizontal velocity.

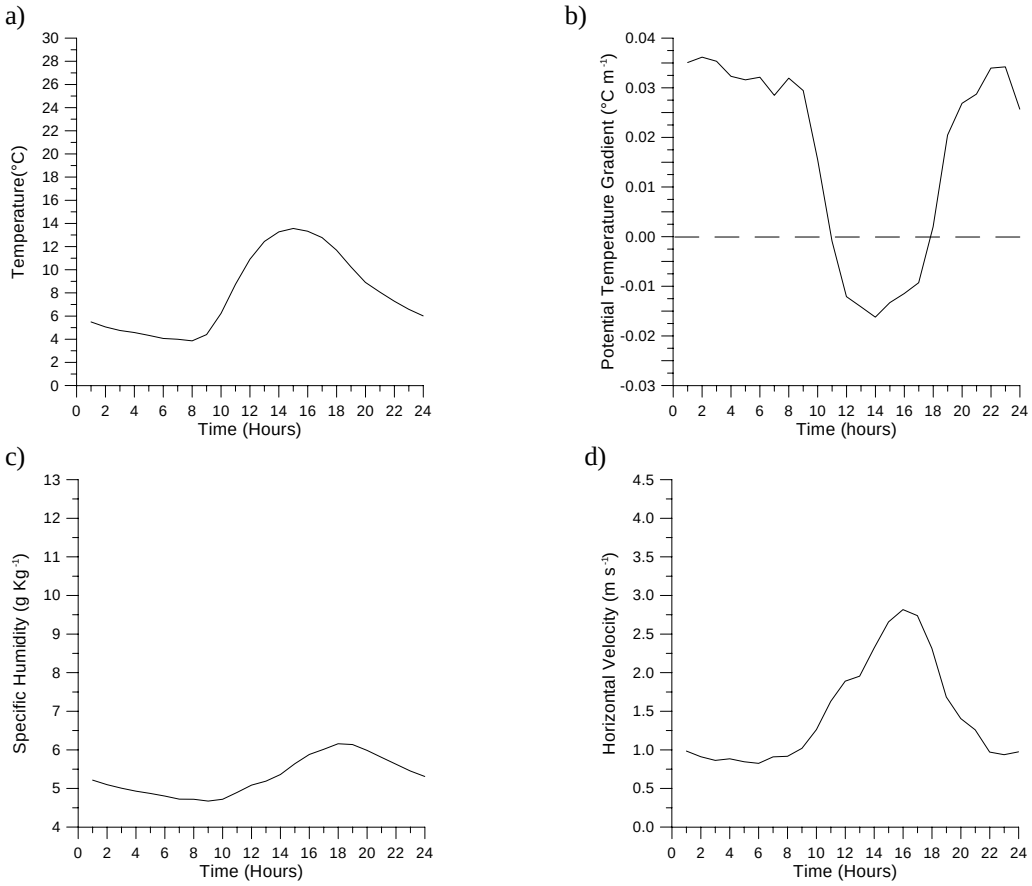

Fig. 7 - Daily cycles in the period January-March 1993; a) temperature, b) potential temperature gradient c) specific humidity and d) horizontal velocity.

stability, the velocity peak of the land breeze can be observed only at high altitudes as will be shown in the next section. It is well known that static stability is not sufficient to determine the flow stability. As a matter of fact, wind shear may produce instabilities.

In order to overcome this limitation, the dynamic stability has been evaluated. By use of the available instrumentation, estimation of the bulk Richardson number [6] can be obtained:

$$R_B = [g\Delta\overline{\theta}\,\Delta z]/[\overline{\theta}[(\Delta\overline{U})^2 + (\Delta\overline{V})^2]], \tag{4.1}$$

in which $\overline{U}$ and $\overline{V}$ are the mean horizontal velocities and $\overline{\theta}$ is the mean potential temperature. The differences Δ have been evaluated between 10 and 30 m levels. In fig. 8a) the results for the period July-September are shown. During the night and the early hours of the morning, stable conditions occur, which attenuate when the land breeze arises. R_B slightly increases when this stops. Immediately afterwards an abrupt drop occurs, R_B becomes negative, namely dynamic instability takes place. The highest

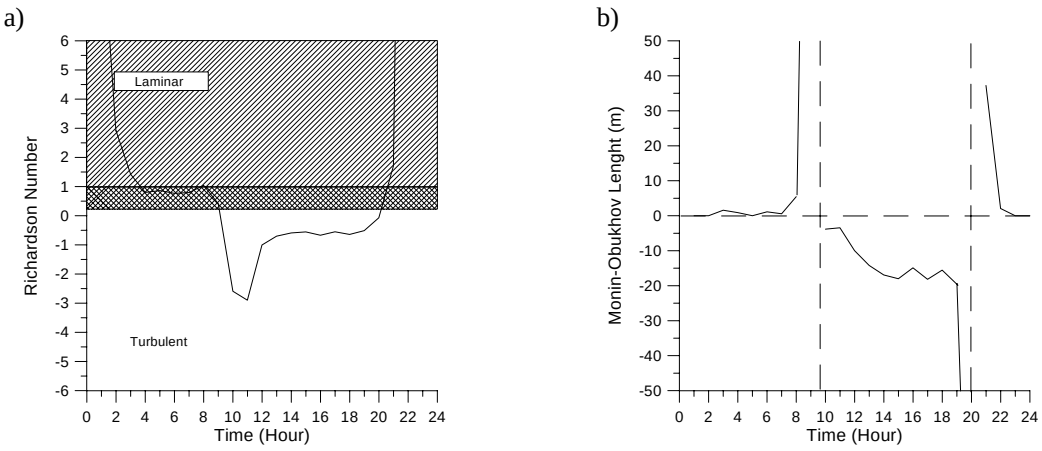

Fig. 8 - Daily cycles in the period July-September 1993; a) Richardson number, b) Monin-Obukhov length.

instability values are reached before the sea breeze reaches its highest levels, because this increases the wind shear term of the turbulent kinetic energy. After sundown temperature gradient reverses as well as the R_B sign. As wind intensity lessens, higher R_B levels are obtained, corresponding to very stable stratifications. It is useful to remember that in the region $1 > R_B > 0.25$ a hysteresis effect occurs, so that, starting from stable condition, the transition to instability occurs for $R_B = 0.25$. While, starting from unstable condition, the transition to stability occurs for $R_B = 1$. Further information on the surface layer can be obtained by the Monin-Obukhov length L. The similarity theory supplies universal profiles for magnitude necessary to calculate dispersion in relation to z/L. The Monin-Obukhov length is proportional to the height below which wind shear prevails over thermic effect. In the case of static stability, Arya [7] assumed the same Monin-Obukhov similarity function $\phi = 1 + 4.7(z/L)$ for both temperature and momentum transfer. As a consequence, the ratio between velocity and temperature scales was equal to $\Delta\overline{M}/\Delta\overline{\theta}$, in which $\overline{M}$ is the mean velocity magnitude. The definition of L with the above assumption leads to [7]

$$L = [u_* \overline{\theta}\, \Delta\overline{M}]/[kg\, \Delta\overline{\theta}], \tag{4.2}$$

where

$$u_* = \left[k\overline{M} - \frac{4.7 kg\, \Delta\overline{\theta} z}{\overline{\theta}\, \Delta\overline{M}}\right] \Big/ \log\left(\frac{z}{z_0}\right); \tag{4.3}$$

$k = 0.4$ is the von Karman constant and z_0 is the roughness length, equal to 0.1 m in the case analysed. For unstable conditions the relation $L = z/R_B$ is used. In fig. 8b) the L diagram for the period July-September is shown. From 0000 to 0800 L is approximately a few meters or zero. The low value of L is a proof again of the strong stable nocturnal stratification and of the fact that starting from a few meters a thermic turbulent effect

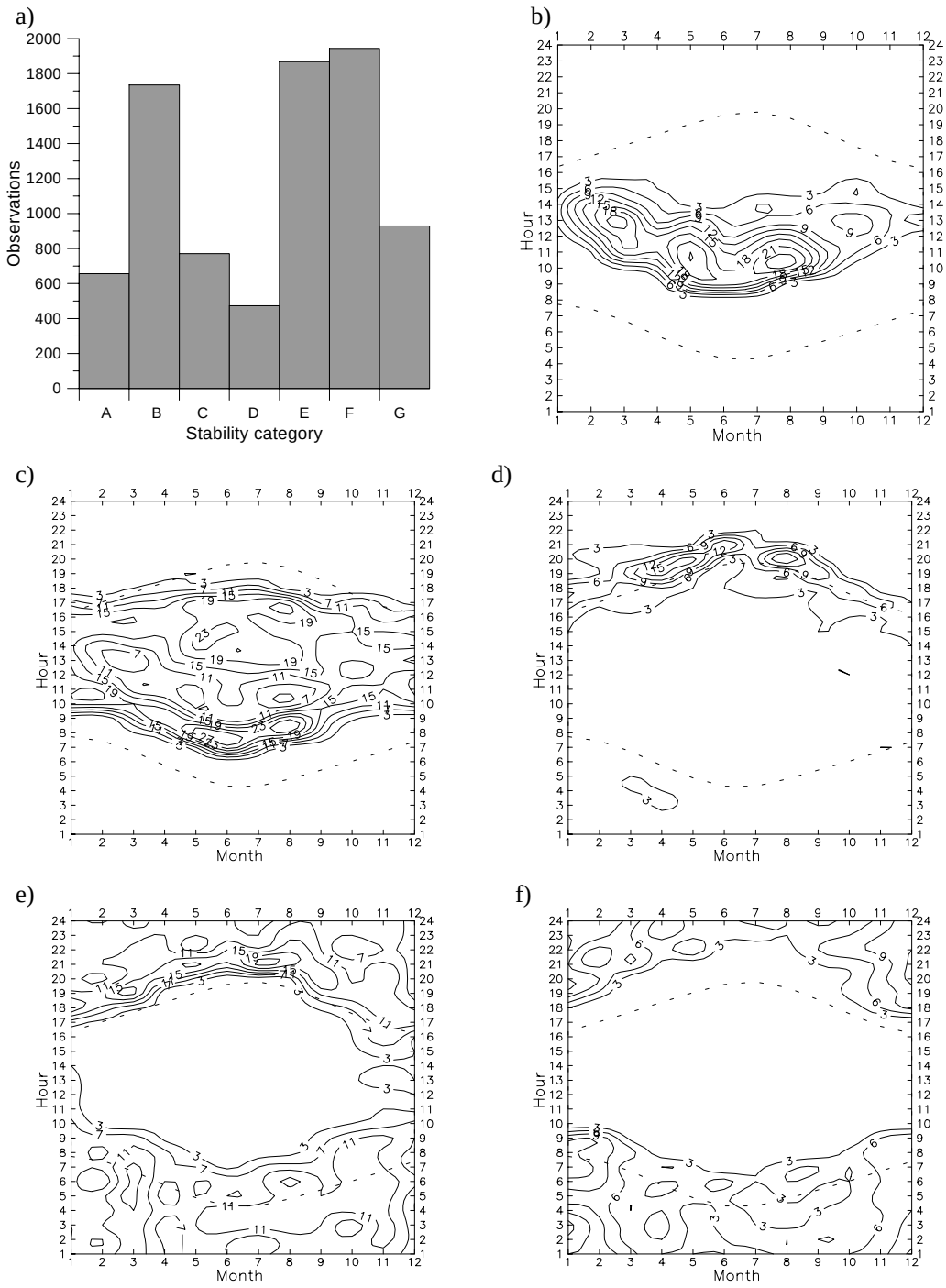

Fig. 9 - Stability categories in the year 1993; a) frequency histogram, b) frequency contours of category A, c) frequency contours of category B, d) frequency contours of category D, e) frequency contours of category E and f) frequency contours of category G.

prevails. When the temperature gradient is zero L has an infinite value and discontinuity occurs, because the gradient changes sign. L reaches a small negative value and in the first warm hours it increases again as does the sea breeze. After sundown L discontinuity occurs again, going from negative infinite values to positive ones. In this case after the first few hours, in which L assumes high values, it drops rapidly.

To estimate the diffusive characteristics of ABL, Pasquill stability categories may be used. In the case where Gaussian models are used, stability categories supply a data base needed to calculate dispersion coefficients. In spite of the backwardness of these models, they are widely employed in the applications. During the daytime, when solar radiation is above 100 W/m^2, the stability category is found by means of the Smith scheme [8]. To make use of the same scheme for night hours, knowledge of cloudiness (in octaves) would be needed but it is not measured by the station, therefore the stability categories have been related to the potential temperature gradient [9]. The histogram in fig. 9a) shows the frequency of the seven Pasquill stability categories. More than 57% of the observations concern stable cases (categories E, F and G), with an absolute maximum of 23% for F category (moderate stability). Only in 36% of the cases the atmosphere is unstable (categories A, B and C), with a relative maximum of 20% for B category (moderate instability). The least frequent is D category (neutral stability) in correspondence with which the buoyancy effects are irrelevant. Figures 9b)-f) show the isofrequency curves, according to the month and the time of day, for some stability categories. Category A (fig. 9b)) is limited only to daytime. In the winter period the maximum line coincides with the hours of major sunlight (1200–1500), whilst in the summer months maximum values are concentrated in the first hours of the morning. Sea breeze, more intense in summer than in winter, produces, from 1200 onwards, an increase in the horizontal velocity module above 3 m/s, maximum limit for A category. In these conditions B category prevails (fig. 9c)) more extensively than the preceding one, which includes conditions of strong solar radiation and strong wind, up to 5 m/s. D category (fig. 9d)) is limited to sundown hours (residual boundary layer) when thermic forcing generated by solar radiation is spent. In these conditions turbulence is produced exclusively by wind shear. E and G categories are peculiar to the night-time, when the vertical gradient of the potential temperature goes from negative values (unstable atmosphere) to positive ones. The graphic area concerned with slight stability E (fig. 9e)) is practically complementary to B category. This shows the maximum line for the early hours of the night when, starting from the ground, the inversion layer begins to erode the residual boundary layer. As time goes on the temperature gradient becomes more intense, so that situations of moderate stability (F category) start to appear. G category (fig. 9f)) is the rarest of the stable situations since the gradient is greater than 0.04 °C/m very infrequently.

4˙2. *Sodar measurements.* – The return signal corresponding to each burst has been processed by a sodar system. If the signal-to-noise ratio S/N was less than 0.75, the data was discarded. Furthermore, if the percentage of discarded data in a period of 10′ was greater than 90%, the mean velocity was rejected. This procedure was carried out for each antenna but the velocity vector could not be constructed, if one of the components was unknown. In fig. 10 the validation rate of the velocity vector, in the period July-September, is drawn. The highest values occur during daytime, when the backscatter of the acoustic waves produced by the turbulence is strong. Anyway, the validation rate above 600 m was often less than 5%. The echo intensity received on 3 August 1993 is shown by the “facsimile” in fig. 11. In the early morning the mixed

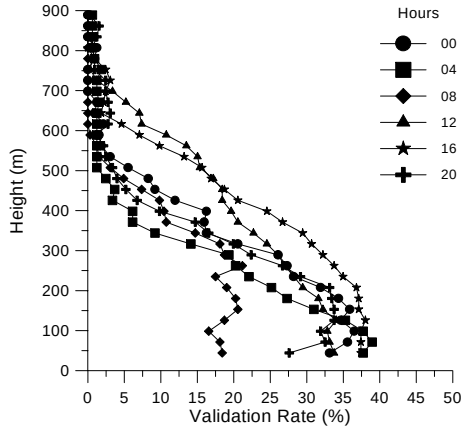

Fig. 10 - Validation rate of the velocity vector measured by sodar, in the period July-September 1993.

layer depth rapidly increases until the sea breeze arrives. Afterward, thermal growth is prevented and convection is confined below 350 m.

In figs. 12a)-f) and figs. 13a)-f) vertical profiles and daily cycle averaged in the periods July-September and January-March are drawn, respectively. During daytime, the horizontal velocity does not vary with the altitude because of the mixing effect; on the contrary, during the night the stable stratification produces a vertical gradient. In the summer time (fig. 12b)) the nocturnal horizontal velocity is enhanced by the land breeze. Such an effect is more evident at high quota and is difficult to recognise by mast anemometers. The vertical velocity is positive until the sea breeze is well established. Development of the sea breeze vortex later produces a downward motion (see Mastrantonio *et al.* [3]) more intense as the height increases. The vertical velocity variance increases during the hot hours, but its maximum value occurs before the solar

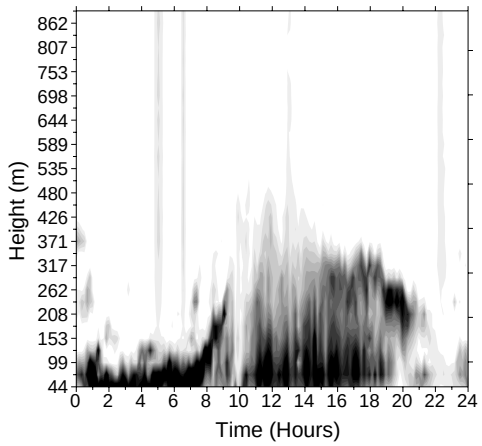

Fig. 11 - Sodar facsimile on 3 August, 1993.

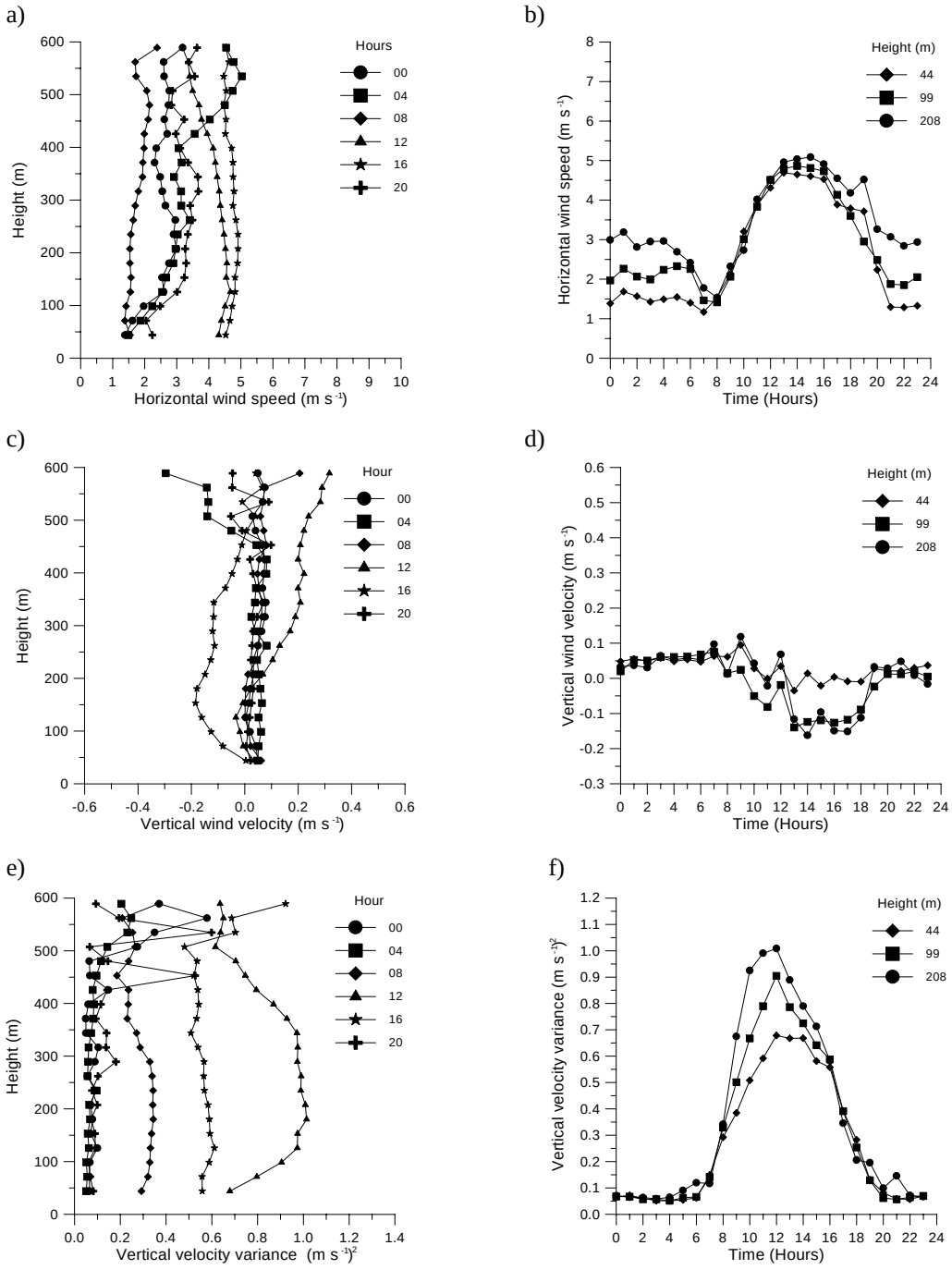

Fig. 12 - Averages of sodar measurements in the period July-September 1993; a) vertical profiles of the horizontal velocity, b) daily cycle of the horizontal velocity, c) as in a) but for the vertical velocity, d) as in b) but for the vertical velocity, e) as in a) but for the vertical velocity variance and f) as in b) but for the vertical velocity variance.

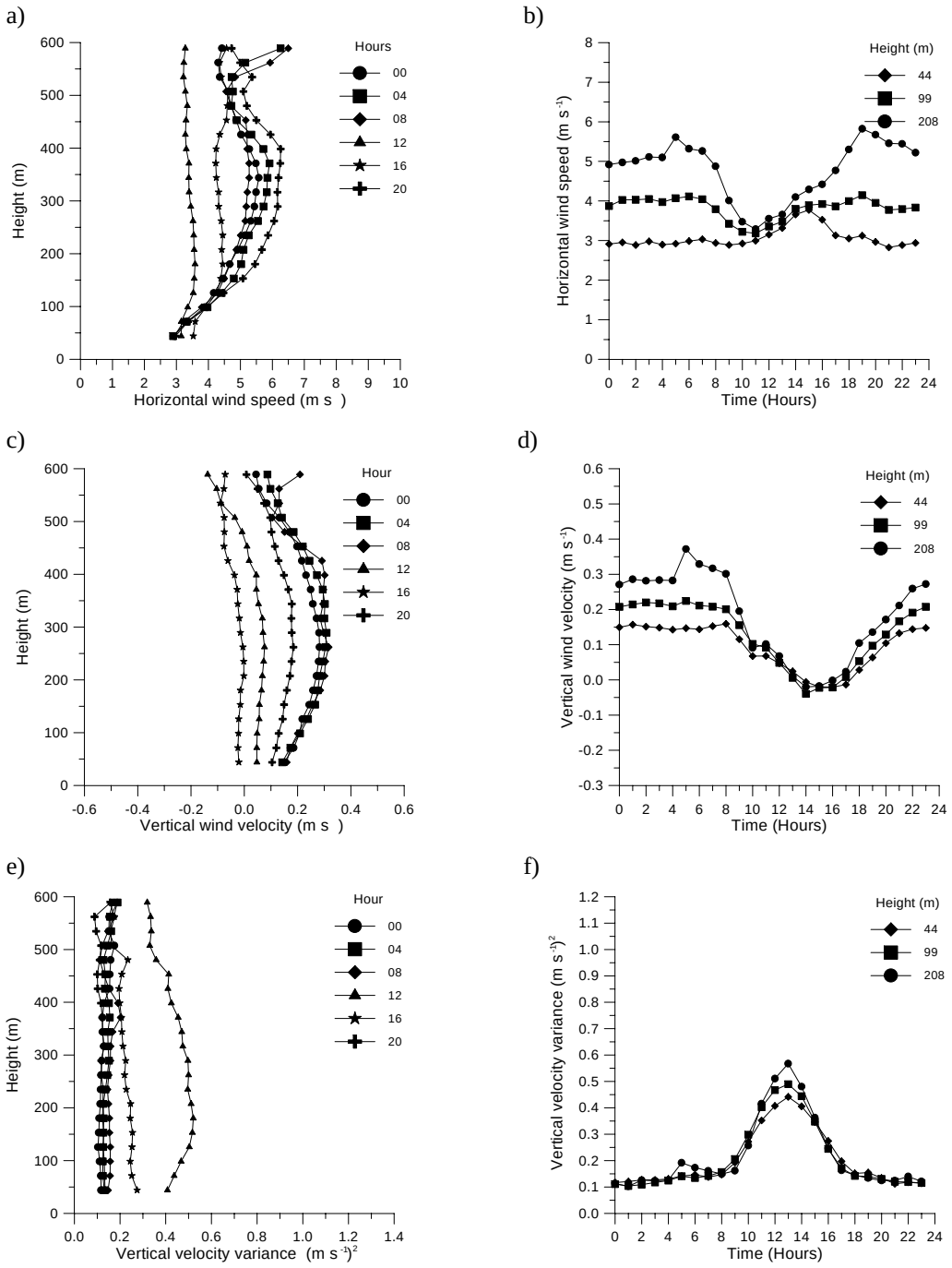

Fig. 13 - Averages of sodar measurements in the period January-March 1993; a) vertical profiles of the horizontal velocity, b) daily cycle of the horizontal velocity, c) as in a) but for the vertical velocity, d) as in b) but for the vertical velocity, e) as in a) but for the vertical velocity variance and f) as in b) but for the vertical velocity variance.

radiation one, because of sea breeze cooling. The vertical profile at 1200 reproduces the typicalbehaviour of the mixed layer. At night-time turbulence is suppressed by the stable stratification. Less obvious phenomena take place during winter. As a matter of fact, the horizontal velocity is almost double during the night with respect to the diurnal values. Such an effect might be due to an overlapping of the synoptic winds and of local circulation, induced by the thermal gradient perpendicular to the shore line. Often the sea temperature is higher than the inland one and the winter winds blow from the east sector (see fig. 5a)). During the daytime the mixed layer increases the drag, furthermore the ground heating reduces the thermal gradient and the velocity drops. The vertical velocity is nearly always positive and assumes non-negligible values. Such an aspect seems to be partially due to the local circulation. A more detailed description of this complex phenomenon would require knowledge of the influence of the urban heat island of the Rome area and other geographic effects.

5. – Analysis of the conditionally sampled results

A further analysis on sea and land breezes has been made. Each day has been tested looking for the occurrence of breezes. The recognition of these events was performed by extending the criteria proposed by Prezerakos [4] to study pure sea breeze. In particular, to select sea breezes the following sequential conditions on wind direction have to be verified:

a) At 0300 and 0500 it must be greater than 330° or less than 130°.

b) In the period 1300–1600 it must be between 150° and 310°.

c) At 0200 of the successive day it must be greater than 330° or less than 130°.

By an analogous procedure, land breezes have been detected:

a) At 1400 and at 1800 the wind direction must be between 150° and 310°.

b) In the period 0200–0500 of the successive day it must be greater than 330° or less than 130°.

c) At 1300 it must be between 150° and 310°.

With these conditions 140 sea breeze days and 126 land breeze days took place during 1993. Including also the conditions on wind velocity magnitude proposed by Prezerakos [4], the sampled days do not show appreciable changes.

Sodar vertical profiles observed during sea and land breeze events have been grouped and separately averaged. Figure 14 shows the average profiles at 1600 during the occurrence of sea breezes and the analogous results at 0500 during land breezes. The averages obtained by sampling the days in which sea and land breezes do not occur are also showed. The horizontal velocity profiles at 1600 (fig. 14a)) are affected by the occurrence of the sea breeze. Below 150 m the profile corresponding to no sea breeze days shows a strong velocity gradient. On the contrary, during sea breeze events the velocity is nearly constant and assumes lower values. In both cases the average profiles are influenced by the frequent occurrence of mixed-layer conditions. A more pronounced velocity difference between profiles takes place at 0500 (fig. 14b)). The velocity gradients in the lower layer are quite similar but the velocity magnitude during land breeze is almost half the complementary case. During daytime the average vertical velocity is negative in correspondence of sea breeze days (fig. 14c)) while it is

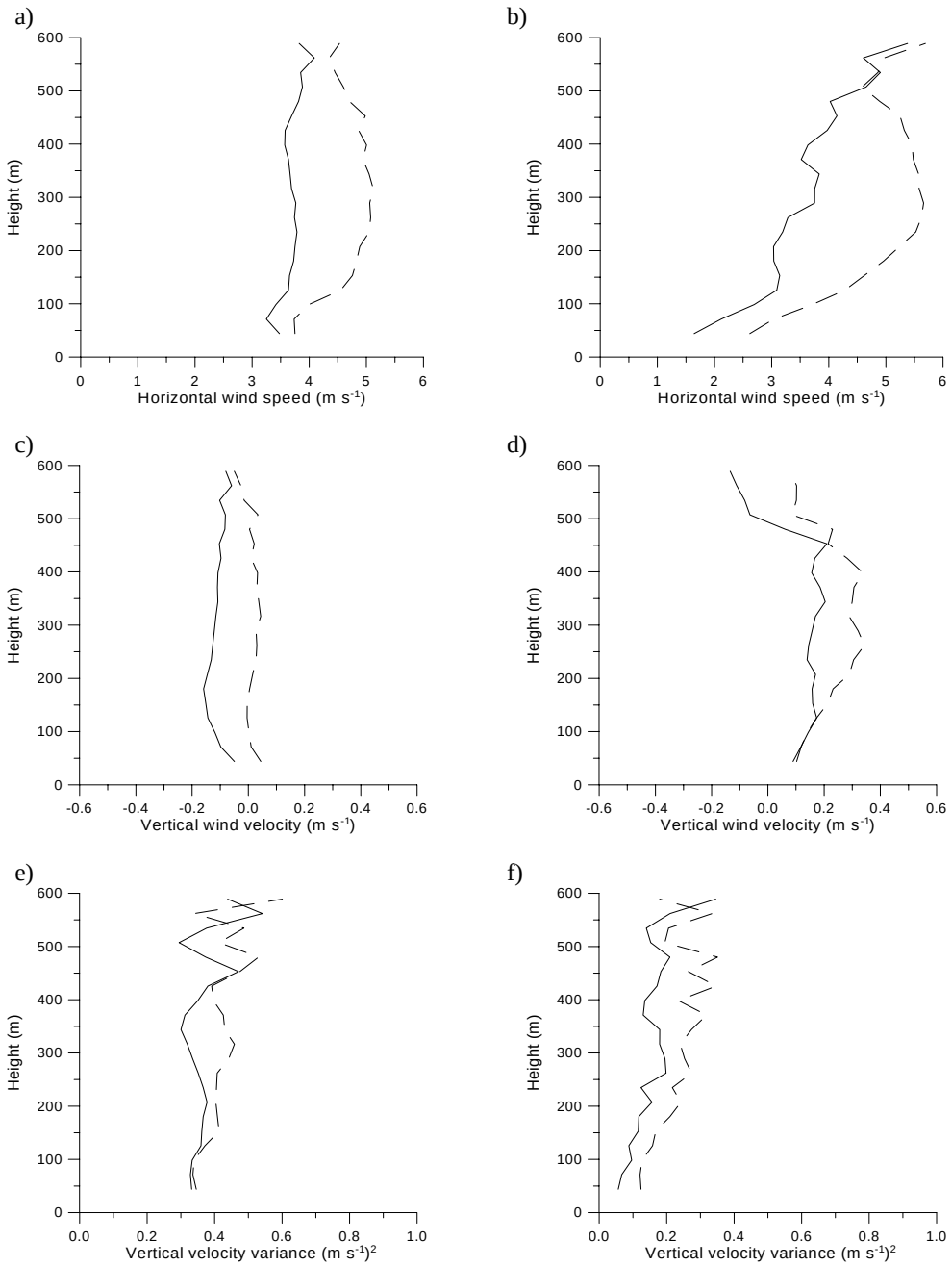

Fig. 14 - Conditionally averaged profiles of sodar measurements during breeze events (continuous line) and no breeze events (dashed line); a) vertical profiles of the horizontal velocity during sea breeze and no sea breeze events at 1600, b) vertical profiles of the horizontal velocity during land breeze and no land breeze at 0500, c) as in a) but for the vertical velocity, d) as in b) but for the vertical velocity, e) as in a) but for the vertical velocity variance and f) as in b) but for the vertical velocity variance.

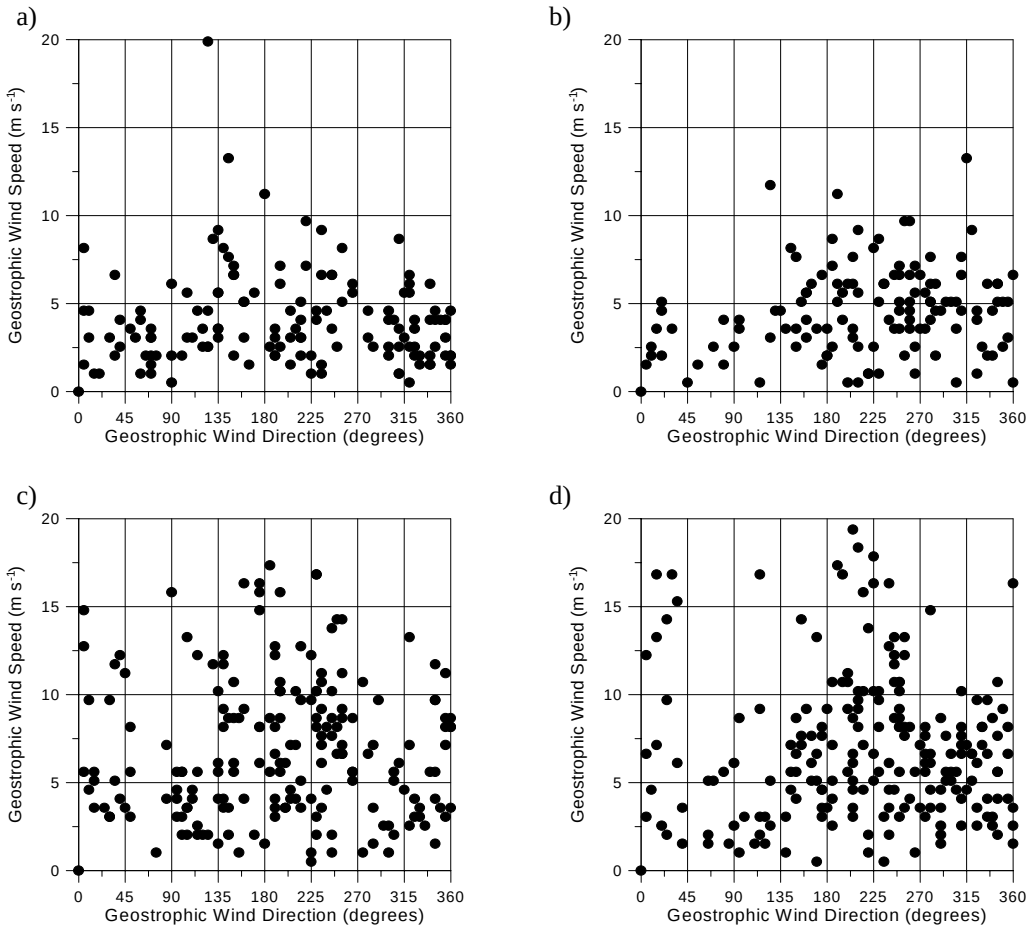

Fig. 15 - Conditionally sampled values of geostrophic wind speed and direction, at 850 mb, during events of : a) sea breezes (at 1200), b) land breezes (at 0000), c) no sea breezes (at 1200) and d) no land breezes (at 0000).

close to zero when the breeze does not arise. At 0500 the vertical velocity is positive apart from the occurrence of land breeze (fig. 14d)). Moreover, vertical velocities are greater if the nocturnal breeze does not occur. As mentioned in the previous section, the explanation of such behaviour is not clear. The variance of the vertical velocity (figs. 14e)-f)) is lower during breeze events. In particular, the profiles are coincident in the layer below 120 m during daytime, revealing a probable dependence on solar radiation rather than sea breeze.

The frequency of the occurrence of breezes can be correlated with the direction and strength of the geostrophic wind. Figure 15 shows the direction and velocity of the wind at 850 mb in correspondence to breeze events during 1993. Also in this case both breeze and no breeze days have been depicted. The number of samples is not sufficient to provide a good statistic accuracy, nevertheless some consideration can be desumed. Above 10 m/s sea and land breeze events are very improbable (figs. 15a), b)), but up to

this threshold both breeze and no breeze cases are present (figs. 15c), d)). As a consequence, the geostrophic wind strength itself cannot furnish a valid prediction tool for the occurrence of breezes. The more frequent geostrophic winds blow from the sector 180°–360°, but perhaps because of the inaccurate statistics, preferential directions for the establishment of breezes do not seem to exist.

6. – Conclusions

In this work some features of the sea and land breeze circulation have been investigated, by means of a 30 m mast and Doppler sodar. From the analysis of the results, the following conclusions may be derived:

1) The vertical velocity and the specific humidity can also be used as indicators of breeze circulation.

2) The maximum instability occurs about 2 hours before maximum solar radiation.

3) The mixer layer depth is reduced by sea breeze.

4) During summer, because of sea breeze circulation, the vertical velocity is negative in daytime.

5) During winter the nocturnal horizontal velocity is almost twice the diurnal one and the winds blow nearly always from the inland.

6) In more than 30% of the days of 1993 sea and land breezes occur. Average profiles during these phenomena show peculiar characteristics.

7) The threshold on the magnitude of the geostrophic wind is not sufficient to predict the breeze events.

* * *

The authors are thankful to AMA for allowing use of their dataset, to Prof. A. CENEDESE for his helpful comments, to Drs. G. MASTRANTONIO and S. ARGENTINI for their suggestions in the analysis of the sodar data.

REFERENCES

[1] HELMIS C. G., ASIMAKOPOULOS D. G., DELIGIORGI D. G. and LALAS D. P., *Boundary-Layer Meteorol.*, **38** (1987) 395.
[2] CHIBA O., *Boundary-Layer Meteorol.*, **65** (1993) 181.
[3] MASTRANTONIO G., VIOLA A. P., ARGENTINI S., FIOCCO G., GIANNINI L., ROSSINI L., ABBATE G., OCONE R. and CASONATO M., *Boundary-Layer Meteorol.*, **71** (1994) 67.
[4] PREZERAKOS N. G., *Boundary-Layer Meteorol.*, **36** (1986) 245.
[5] KAGA A., YAMAGUCHI K., INOUE Y., KONDO A. and LEE H. W., in *Experimental and Numerical Flow Visualization*, *FED*, Vol. **218,** edited by B. KHALIGHI, T. KOBAYASHI, D. H. FRUMAN, M. J. BRAUN, C. J. FREITAS and F. BABAN, 1995, pp. 139-143.
[6] STULL R. B., *An Introduction to Boundary Layer Meteorology* (Kluwer Academic Publishers, Dordrecht) 1988, pp. 177-179.
[7] ARYA S. P. S., *J. Appl. Meteorol.*, **20** (1981) 1192.
[8] SMITH F. B., Meteorol. Office, Turbulence and Diffusion Note No. 40 (1973).
[9] U.SA.E.C., Safety Guide 23, Washington, D.C. (1972).